

# HENRY

Hydraulic Engineering Repository

Ein Service der Bundesanstalt für Wasserbau

---

Conference Paper, Published Version

**Isserty, Guillaume; Walther, Régis; Bertrand, Olivier**  
**3D hydrosedimentary models of the Loire Estuary using**  
**TELEMAC-3D-TOMAWAC and GAIA**

Zur Verfügung gestellt in Kooperation mit/Provided in Cooperation with:  
**TELEMAC-MASCARET Core Group**

---

Verfügbar unter/Available at: <https://hdl.handle.net/20.500.11970/110851>

Vorgeschlagene Zitierweise/Suggested citation:

Isserty, Guillaume; Walther, Régis; Bertrand, Olivier (2022): 3D hydrosedimentary models of the Loire Estuary using TELEMAC-3D-TOMAWAC and GAIA. In: Bourban, Sébastien E.; Pham, Chi Tuân; Tassi, Pablo; Argaud, Jean-Philippe; Fouquet, Thierry; El Kadi Abderrezzak, Kamal; Gonzales de Linares, Matthieu; Kopmann, Rebekka; Vidal Hurtado, Javier (Hg.): Proceedings of the XXVIIIth TELEMAC User Conference 18-19 October 2022. Paris-Saclay: EDF Direction Recherche et Développement. S. 153-161.

**Standardnutzungsbedingungen/Terms of Use:**

Die Dokumente in HENRY stehen unter der Creative Commons Lizenz CC BY 4.0, sofern keine abweichenden Nutzungsbedingungen getroffen wurden. Damit ist sowohl die kommerzielle Nutzung als auch das Teilen, die Weiterbearbeitung und Speicherung erlaubt. Das Verwenden und das Bearbeiten stehen unter der Bedingung der Namensnennung. Im Einzelfall kann eine restriktivere Lizenz gelten; dann gelten abweichend von den obigen Nutzungsbedingungen die in der dort genannten Lizenz gewährten Nutzungsrechte.

Documents in HENRY are made available under the Creative Commons License CC BY 4.0, if no other license is applicable. Under CC BY 4.0 commercial use and sharing, remixing, transforming, and building upon the material of the work is permitted. In some cases a different, more restrictive license may apply; if applicable the terms of the restrictive license will be binding.

Verwertungsrechte: Alle Rechte vorbehalten

# 3D hydrosedimentary models of the Loire Estuary using TELEMAC-3D-TOMAWAC and GAIA

Guillaume Isserty<sup>1</sup>, Régis Walther<sup>1</sup>, Olivier Bertrand<sup>1</sup>

guillaume.isserty@arteliagroup.com

<sup>1</sup>: ARTELIA, 6 rue de Lorraine, 38130 Echirolles, France

**Abstract** – Supervised by the Loire Estuary Public Interest Group (GIPLE), 3D hydrosedimentary models were built and calibrated to provide answers at the scale of estuary, for several physical processes: hydrodynamics conditions, mud dynamics, water quality, dumping and dredging processes. These models take full advantage of the GAIA module in TELEMAC, and shows its ability to provide good results of complex processes at a large scale. This paper presents the building and calibration steps for 2 of the models developed: the global hydrosedimentary model, and the local dumping model. Water quality, and dredging processes modelling is still an ongoing work.

**Keywords:** estuaries, sediment processes, maritime, sandy-mud mixtures, salinity.

## I. INTRODUCTION

The Loire estuary is one of the three major French estuaries. It is a macro-tidal estuary with a mean spring tidal range of about 5 m allowing the tide to propagate up to Ancenis, 90 km upstream from the mouth (Saint-Nazaire). The water quality of the estuary is considered as relatively bad with a large maximum turbidity due to significant developments over the two last centuries including a deep-water port development downstream in the Saint-Nazaire area with an outer navigation channel down to -12.5m Chart Datum and the creation of a unique inner navigation channel at -5m CD up to the city of Nantes located 55 km upstream from Saint-Nazaire. Large scale hydrosedimentary modelling can be a great decision making tool for any stakeholder in such estuary, whether it is to properly manage the cities drinking water supply, to assess the filling rate of navigation channels... To that extent, several 3D numerical models were built under the supervision of the Loire Estuary Public Interest Group (GIPLE) using TELEMAC3D coupled with GAIA and TOMAWAC. These models provide an update of the existing ones on the estuary, which were set up in 2012. It will take full advantage of the GAIA module which was not available at that time. The global model was calibrated for each of the main processes that occur in the estuary. A more local and specific model for sediment dumping was also developed. A third model is still being developed in which we model the dredging processes of the estuary, along with dumpings and dispersion of sediments.

## II. GLOBAL HYDROSEDIMENTARY MODEL

The goal of the global hydrosedimentary model is to solve global scale hydrodynamics and sedimentary processes inside the estuary. Water levels, salinity and sediment

transport are at stake and the hydrosedimentary model will be the basis for the other models. All the different processes modelled may impact one on each other. It was thus decided to calibrate the model in a “step-by-step” way, adding processes one after another, starting with simple hydrodynamics, and ending with fully coupled hydrosedimentary model, including wave effects.

### A. Extent, bathymetry and mesh

The global hydrosedimentary model extends from a marine boundary more than 100 km from the coast to the upstream boundary located roughly 100 km upstream inside the estuary. The marine boundary is located far enough away to limit the suspended sediment concentration exit from the model. The upstream boundary is located above the tide effects upward limit.

The model bed elevations are based on several bathymetric sources. They were aggregated carefully to avoid gaps or jumps at the connections. Inside the estuary, the bathymetry available has fine resolution (around 1 meter). Outside, bathymetry from HOMONIM project is used (50 meters resolution).

Final mesh has 50,000 2D nodes, and 12 vertical planes, leading to roughly 650,000 3D nodes. The vertical planes are a mix between fixed elevation planes and sigma planes. If the water levels are low, the vertical mesh is made of only sigma planes. This will allow good representation of stratification phenomena, whatever the hydrodynamics conditions. Global scale model bathymetry is shown in Figure 1.

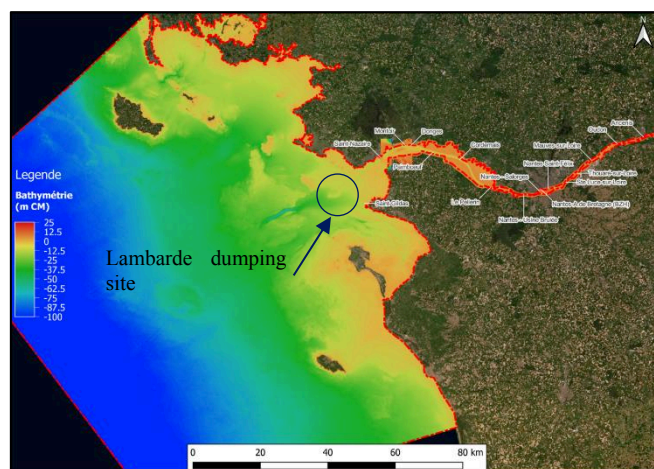


Figure 1. Global scale model bathymetry

## B. Hydrodynamics

At first, only hydrodynamics is modelled and calibrated.

### 1) Stakes and goals

The modelled area is subject to semi-diurnal tide. The upstream border location was set up to be the tide influence limit. Regarding river flows, Loire has the highest contribution by far. Two of its tributaries are also present in the Nantes city area.

During floods, the flow can reach around 6,000 m<sup>3</sup>/s, while in extreme low-waters it can decrease down to 60 m<sup>3</sup>/s. Mean annual flow is around 800 m<sup>3</sup>/s.

Competition between tide and river flow has to be well modelled to ensure proper results regarding salinity, SSC or water quality.

### 2) Numerical implementation

#### a) Tide and river flow forcing

At the downstream maritime boundary, astronomical tide is reconstructed from 32 waves extracted from FES2012 model [5]. At the upstream boundary, the combined Loire and Evre discharges are imposed. Inside the model, two of the Loire tributaries river rates discharges are imposed in source points.

#### b) Meteorological forcing

Pressure effects are taken into account thanks to temporal variation of the mean sea level at the maritime boundary. Wind temporal and spatial variation are imposed on the whole model. Data is extracted from the HOMERE database. Inside the estuary, wind intensity is lowered, up to a certain point where it is set to zero. From this point, the shading by buildings or vegetation is too pronounced to account for wind effects.

#### c) Friction coefficient

Friction coefficient is variable in space, and time, as a function of the upstream flowrate. A Nikuradse friction coefficient is used. Fluid mud plays an important role for the friction inside the estuary and is therefore taken into account.

Depending of the flowrate, the fluid mud is located rather upstream or downstream in the estuary. Lateral and longitudinal limits need to be calibrated. The Nikuradse friction coefficient is lowered to 0.00087 m for the fluid mud parts. This value comes from lab experiments that were made on Loire muds [2].

#### d) Calibration methodology

Six different periods are chosen for calibration. They are each representative of a particular flowrate. During these periods, we mainly focus on a 24 hours period during which flowrate is quite constant, and we calibrate bottom friction coefficient and fluid mud position to match the measured water-levels all along the estuary.

Calibration validity is controlled thanks to root mean square error, mean error and standard deviation, along with three other time percentage parameters which are presented in the Table I.

Table I – Definition of CF, POF, COF

<b>CF(X)</b>	Percentage of errors inside [-X;X]
<b>POF(X)</b>	Percentage of errors over X
<b>NOF(X)</b>	Percentage of errors below -X

The calibration is considered good if CF(X) is above 90% during the 24 hours period, with X set to 0.2 meters. Results are also compared on the whole period (2 weeks) to ensure that they have the same quality. The calibration results in a set of friction coefficient and mud positions for each of the 6 flowrates. For the simulations these values are interpolated linearly for every flowrate.

This method is finally validated on three long-term periods of three months each, representative of different hydrodynamic conditions.

### 3) Results and discussion

#### a) Friction coefficient map

Friction coefficient and mud positions are calibrated (see II.B.2)c). Table II summarizes mud positions (indicated in kilometric point (KP) from the estuary mouth) as a function of flowrate.

Table II – Mud position as a function of upstream flowrate

Flowrate (m <sup>3</sup> /s)	125	200	400	850	2500	4000
Downstream limit (KP <sup>7</sup> )	17.6	13	10	2	-5	-5
Upstream limit (KP)	65	50	35	22	13	11

A total of 15 gauge stations are used for this calibration phase. The resulted friction coefficients are shown in Figure 2. Friction values are summarized at every gauge stations available. In addition, the Downstream Limit (DL) and Upstream Limit (UL) of fluid mud are added.

<sup>7</sup> Kilometric Point from Saint-Nazaire harbour

Nom	Flowrate KP (km)	Friction coefficients (in m)					
		4000 m <sup>3</sup> /s	2500 m <sup>3</sup> /s	850 m <sup>3</sup> /s	400 m <sup>3</sup> /s	200 m <sup>3</sup> /s	125 m <sup>3</sup> /s
Downstream limit of navigation channel	-15	0.002	0.002	0.002	0.002	0.002	0.002
DL(4000)/DL(2500)	-5	0.00087	0.00087				
Saint-Nazaire	-0.5	0.00087	0.00087	0.05	0.05	0.002	0.002
DL(850)	2	0.00087	0.00087	0.00087			
Montoir	7.9	0.00087	0.00087	0.00087	0.05	0.002	0.002
Donges	9.4	0.00087	0.00087	0.00087	0.002	0.002	0.002
DL(400)	10	0.00087	0.00087	0.00087	0.00087		
UL(4000)	11	0.00087	0.00087	0.00087	0.00087		
UL(2500)/DL(200)	13		0.00087	0.00087	0.00087	0.00087	
Paimboeuf	16.4	0.002	0.05	0.00087	0.00087	0.00087	
DL(125)	17.6			0.00087	0.00087	0.00087	0.00087
UL(850)	22			0.00087	0.00087	0.00087	0.00087
Cordemais	24.7	0.15	0.05	0.15	0.00087	0.00087	0.00087
UL(400)	35				0.00087	0.00087	0.00087
Le Pellerin	37.7	0.15	0.1	0.15	0.05	0.00087	0.00087
Nantes - Usine Brûlée	48.1	0.2	0.2	0.15	0.1	0.00087	0.00087
UL(200)	50					0.00087	0.00087
Nantes - Salorges	53	0.2	0.2	0.2	0.15	0.15	0.00087
Nantes - A. de Bretagne	53.5	0.2	0.2	0.25	0.15	0.2	0.00087
Nantes - Saint Félix	56	0.2	0.2	0.25	0.15	0.25	0.00087
Sainte-Luce	61.8	0.1	0.1	0.15	0.15	0.3	0.00087
UL(125)	65						0.00087
Thouaré	66.5	0.3	0.4	0.4	0.4	0.3	0.3
Mauves	72.3	0.3	0.2	0.1	0.2	0.2	0.3
Oudon	82.1	0.3	0.2	0.1	0.2	0.1	0.1
Ancenis	90.5	0.3	0.5	0.2	0.15	0.1	0.1
Upstream Boundary	100	0.3	0.5	0.2	0.15	0.1	0.1

Figure 2. Final Nikuradse friction coefficients (in m) for the 6 flowrates

b) Calibration and validation results

A good calibration (CF(0.2)>90%) was reached for nearly all retained gauge stations and for every time period. RMSE is nearly always below 0.1m. Figure 3 shows graphical comparison of water levels evolution at a station located rather upstream inside the estuary. The model is particularly able to reproduce correctly the period if river flow influence is greater than tide influence. Scores of the model are summarized for this same station in the scatter plot displayed in Figure 4. Most of the simulated water levels are very close to the measured one. Only for < 10 measurements the deviation is bigger than 0.2 m.

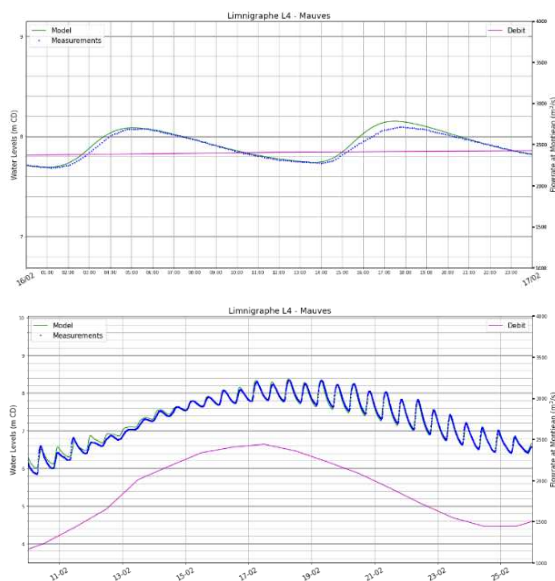


Figure 3. Temporal water levels evolutions for Mauves gauge station. Green line: model results; pink line: flowrate; blue dots: gauge data

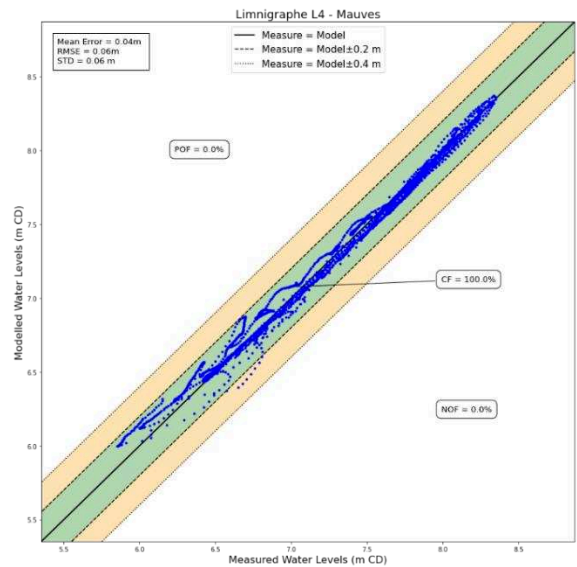


Figure 4. Scatter plot for Mauves gauge station – Calibration period

Validation step was made of three different periods lasting three months each. Hydrodynamics condition were either flood (winter 2021), severe low-waters (summer 2019), or mean conditions (spring 2011). Once again, RMSE was often around 0.1 meters. Comparison can be synthetized in one scatter plot for each gauge station. Figure 5 is an example of a validation result over the 2011 period, at the mouth of the estuary.

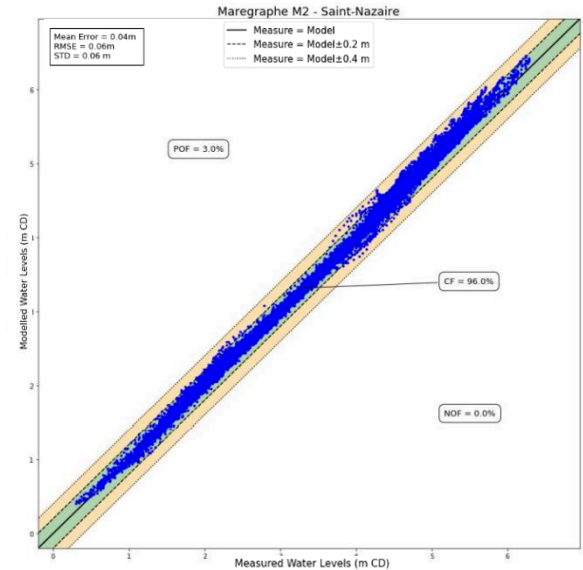


Figure 5. Scatter plot for Saint-Nazaire gauge station – Validation period



### C. Salinity

#### 1) Stakes and goals

Vertical salinity layering in the downstream part of the estuary can be quite significant, especially on extreme hydrodynamics conditions:

- During flood, a high freshwater surface flow is opposed to bottom saline water flow, leading to high stratification
- During low-waters, tidal force is not high enough to mix the water vertically. A two-layer flow (one saline, the other fresh) thus exists, with very little exchanges between them. Density driven flow occur, and as the river flow is too low, it induces high salinity upwell, from the sea towards inner estuary.

A good representation of vertical turbulent diffusion will be necessary to reproduce such phenomena.

#### 2) Numerical implementation

##### a) Vertical turbulence modelling

The turbulence model used for this study is a modification of the standard mixing-length model [7]. It adds a correction based on the grade of stratification. In the standard mixing-length model, a damping function is used to account for stratification effects. The formulation of this function is based on experimental or in-situ data. The main issue with this model is that the height of the main dissipating scale must be given.

In cases where stratification is high enough, turbulent production in the lower layer is independent from production in the upper layer. The mixing length is thus calculated in an independent way in the two layers. If it is not high enough, standard mixing length is used. Schematic of the modification between the two models is shown in Figure 6.

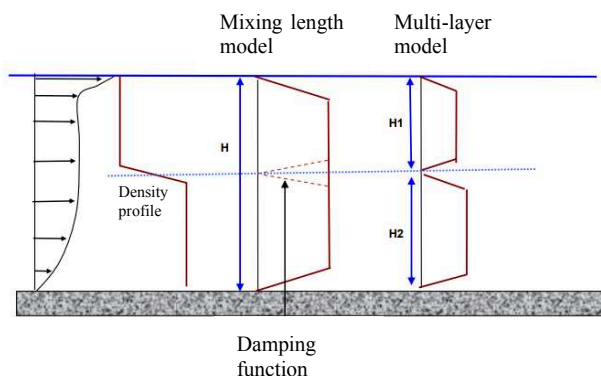


Figure 6. Mixing length and multi-layer vertical turbulence model

The Richardson number is used to consider if stratification is dominant. If the Richardson is above a chosen threshold (typically around 0.2-0.25), stratification dominates, and multi-layer model is used.

The Loire models from 2012 show similar results with this multi-layer model to a k-epsilon model, but with lower computational costs.

#### b) Waves action

In addition to forcing used for the modelling of hydrodynamics, waves parameters have to be computed at each point of the model. The model is forced at its maritime boundary by data from HOMERE database regarding waves: wave height  $H_{m0}$ , peak period  $T_p$ , Peak Direction  $D_p$  and direction spread  $Sp_d$ .

#### 3) Results and discussion

One of the parameters that can be calibrated is the critical Richardson number, which determines if the two layers are considered independent for turbulent production (and mixing length calculation).

Critical Richardson was finally set up to 0.2. Comparison of the model results to available measures is analysed qualitatively, making sure that the model can correctly reproduce the following phenomena:

- Good representation of stratification period, whether it is low-water (with weak vertical mixing, and weak horizontal spread), low flow (with weak vertical mixing, and little opposition to density driven currents going upward), or flood (with freshwater flow in surface, and saline water entering the estuary in the bottom);
- Good representation of mixing periods whether it is spring tide with a strong vertical mixing, and horizontal spreading or a wind blow inducing a strong vertical mix.

The final choice of parameters was made so that the model reproduces as well as possible the saline upwells. These phenomena will be important to also reproduce cohesive sediment upwells for the final hydrosedimentary model. Figure 7 shows the good representation of salinity evolution during a whole year, including two high flowrate periods.

Blue squares in the figure indicates periods where measurements behave strangely. Discrepancies during these periods are not representative of the model performance.

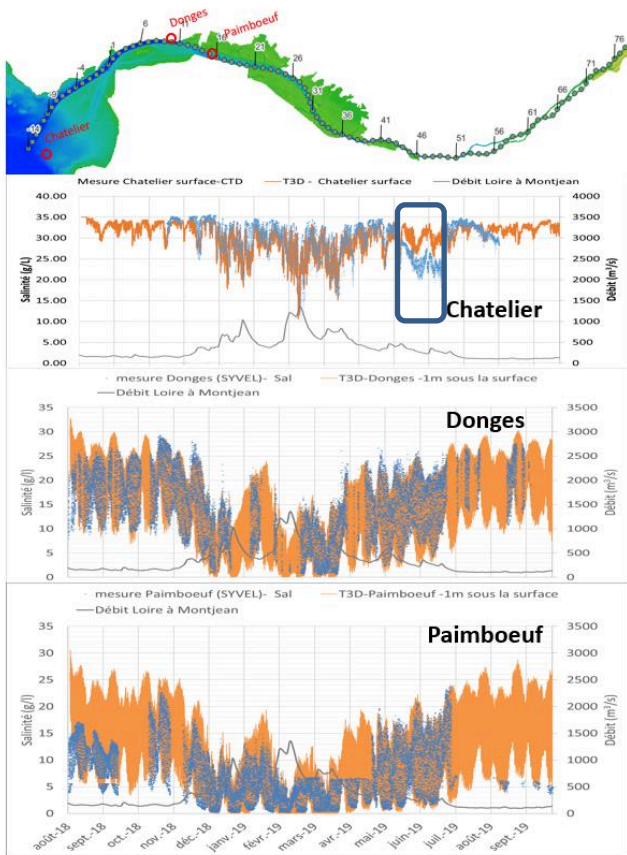


Figure 7. Temporal evolution of salinity – Model (orange) versus measure (blue dots)

#### D. Sediment

##### 1) Stakes and goals

This global scale model is particularly made to reproduce the mud dynamic inside the whole estuary. Parameters that will be of interest are the following ones:

- Suspended matter → temporal and spatial evolution and stratification depending on hydrodynamics conditions
- Fluid mud dynamic → temporal and spatial evolution of the thickness of the different types of fluid mud layers, being:
  - consolidated fluid mud (325 to 375 g/l);
  - Sensu-stricto fluid mud (125 to 300 g/l);
  - Liquid fluid mud (40 to 100 g/l).

##### 2) Physical processes

###### a) Settling Velocity

For the global model, we mainly focus on the mud cap dynamic inside the estuary. Only mud is transported, not sand. The dynamics of this cohesive sediment are determined by solving the transport equation:

$$\begin{aligned} \frac{\partial c}{\partial t} + u \frac{\partial c}{\partial x} + v \frac{\partial c}{\partial y} + w \frac{\partial c}{\partial z} + \frac{\partial W_s c}{\partial z} \\ = \frac{\partial}{\partial x} \left( \varepsilon_x \frac{\partial c}{\partial x} \right) + \frac{\partial}{\partial y} \left( \varepsilon_y \frac{\partial c}{\partial y} \right) \\ + \frac{\partial}{\partial z} \left( \varepsilon_z \frac{\partial c}{\partial z} \right) \end{aligned} \quad (1)$$

The settling velocity  $W_s$  is determined using three different field measurement data. A Thorn/Mehta law [8] is matched to this data. Two different behaviours are observed depending on the concentration. At lower concentrations, the law obtained is in the form

$$W_s = k_1 \times C^{m1} \quad (2)$$

At higher concentrations, flocs induce a velocity decrease. The corresponding law is:

$$W_s = W_{s0} \times (1 - k2 \times C)^{m2} \quad (3)$$

In addition, flocculated or unflocculated state of the flow is simply determined by mean velocity and is taken into account by reducing the settling velocity in case of unflocculated flow.

###### b) Deposition fluxes

At the interface between soil and water, deposition and erosion occur, at rates that need to be determined. According to the theory detailed in [1], consolidation starts when concentration is roughly above 40 g/L. Mass transfer between suspended sediments and the first bottom layer thus occur as soon as the concentration is greater than 40 g/L. The deposition flux is calculated as follows

$$F_{dep} = W_s \times C_{bottom} \quad (4)$$

with  $W_s$  being the settling velocity at the bottom of the water column.

###### c) Mud erosion

An erosion rate law is established for this study, based on measurements from [2] Sanchez.

###### d) Pure sand erosion

In the case of pure sand, transport is calculated using van Rijn transport 2004 model [3] which is not detailed here.

###### e) Mud/sand mixture erosion

In the case of a mixture of sand and mud, the law used is a function of the fraction of mud. If the mud mass fraction inside a sand/mud mixture is below 0.3, the critical erosion shear stress is higher than the one of pure sand. Mud infiltrates inside holes between sand grains and adds cohesion to the mixture. If the fraction is higher than 0.3, sand grains lose contact between each other, and critical erosion shear stress gets lower. Finally, if the fraction is higher than 0.5, the mixture behaves as pure mud.

###### f) Consolidation

The consolidation model uses different sediment layers (16 for our model), each one having a fixed concentration and critical erosion shear stress. Mass transfer between layers is calculated with a simple transfer function:

$$\frac{dm}{dt} = a \quad (5)$$

$a$  being a coefficient that needs to be calibrated for each layer. In our case,  $a$  was determined using [1]. One can find in this paper the solid discharge ( $Q_c$ ) through a constant concentration ( $C$ ) layer:

$$Q_c = VC \left[ A_2 A_1 \left( \frac{C}{\rho_s} \right)^{A_3} - 1 \right] \quad (6)$$

with  $A_1=1.6$  m/s,  $A_2=72$  and  $A_3 = 0.65$  for a Loire mud. This solid discharge corresponds exactly to the mass transfer between two layers and is thus equal to the parameter  $a$  in equation (5).

#### g) Sliding

Without any sliding, sediment tends to settle rapidly in navigation channel banks, and are quite never getting back into suspension, because hydraulic stress is not high enough. In our model, for layers of concentration ranging from 40 to 100 g/l (liquid fluid mud), deposited sediments slide in the direction of the strongest slope, as soon as a critical slope is overpassed. The critical slope chosen in the model corresponds to observations in the Saint-Nazaire port and is equal to 2.5% (1.43°). This sliding process is numerically done within the `gaia_maxslope` routine, modifying the angle value for the considered bed layers (for the previously described concentrations).

### 3) Numerical implementation

#### a) Sediment forcing

Regarding sediment modelling, three different kinds of forcing are used:

- Upstream boundary condition, with a sediment flowrate, reconstructed from available measurement data;
- Bottom boundary condition, with initial composition of the bed layers, based on sediment composition extracted from the EMODnet project [4];
- Initial fluid mud conditions, shown in Figure 8.



Figure 8. Initial fluid mud conditions (mud: green, no mud: blue): liquid fluid mud on the left, stricto-sensus and consolidated fluid mud on the right

#### b) Bed model using GAIA

The bed model is composed of 16 sediment layers between which mass transfer can occur, along with an additional layer which represents the initial sediment composition (based on the EMODnet project) and which is independent from the other layers (i.e. mass-transfer cannot occur). An active layer is also set up at the top.

The sixteen layers are sand and mud mixtures, of different mud concentration. They can be divided into 3 main groups:

- Consolidated fluid mud: 3 layers with concentration ranging from 325 to 375 g/L;
- Sensu-stricto fluid mud: 9 layers with concentration ranging from 125 to 300 g/L;
- Liquid fluid mud: 4 layers with concentration ranging from 40 to 100 g/L.

Mass transfer between layers is calculated thanks to the consolidation model equations detailed before.

### 4) Results and discussion

Figure 9 shows the annual dynamic of SSC inside the inner estuary. The mud cap (concentrations below 40 g/L) signal corresponds well to the one observed in situ by the GIPLE [6]. Its length and intensity vary with tide cycles (strong concentration and big length for high-tides, and the opposite for low-tides), and its core moves upward or downward depending on river flow. When river flow is important, mud cap is contained below kilometric point 25, and when it is very low, it can climb up to Mauves (kilometric point 70).

Model is also compared to several SYVEL (a continuous measurement network) gauge stations measurements of the SSC. The three stations presented in Figure 10 show different mud dynamic depending on longitudinal locations.

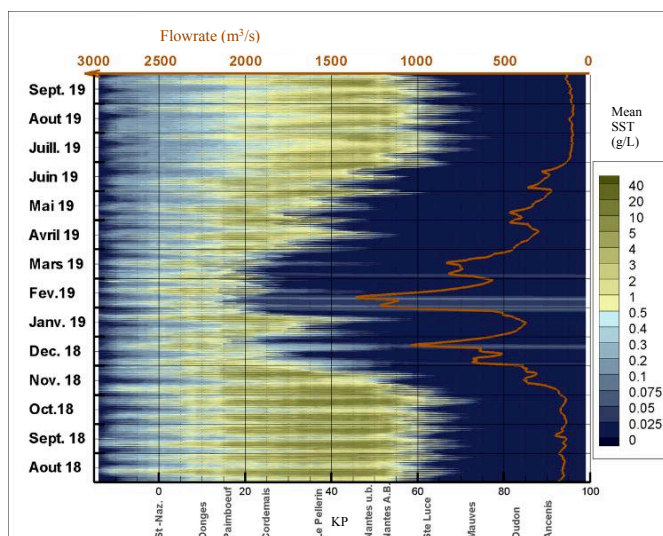


Figure 9. Modelled annual dynamic of SSC



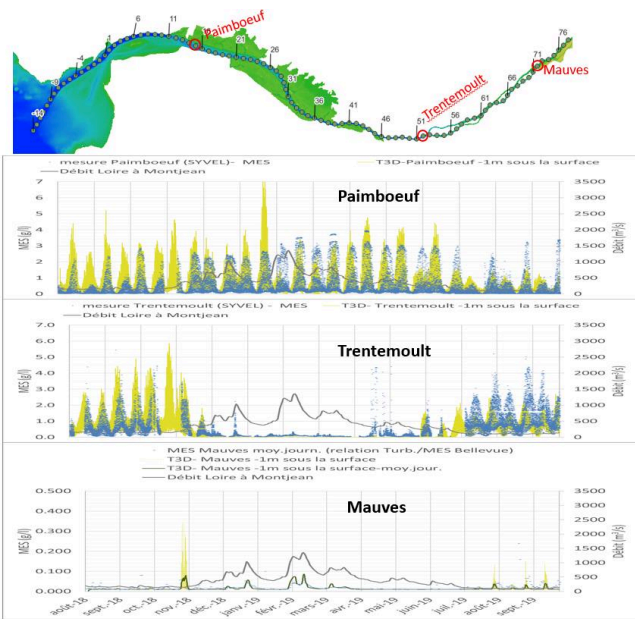


Figure 10. Model results versus SYVEL measurements for SSC

Finally, Figure 11 shows the global fluid mud dynamics. Measurement of fluid mud deposits are regularly performed by the port authority along the navigation channel. The analysis of these data indicates that there is no mud in the channel navigation upstream of the kilometeric point 30 for a discharge of 500 m<sup>3</sup>/s (mean discharge of the ten last days). This phenomenon is reproduced with the numerical model during a one year simulation. We can see on Figure 11 that during flood conditions the mud is located downstream and then moves up to the kilometeric point 30 when the discharge of the ten last days is less than 500 m<sup>3</sup>/s.

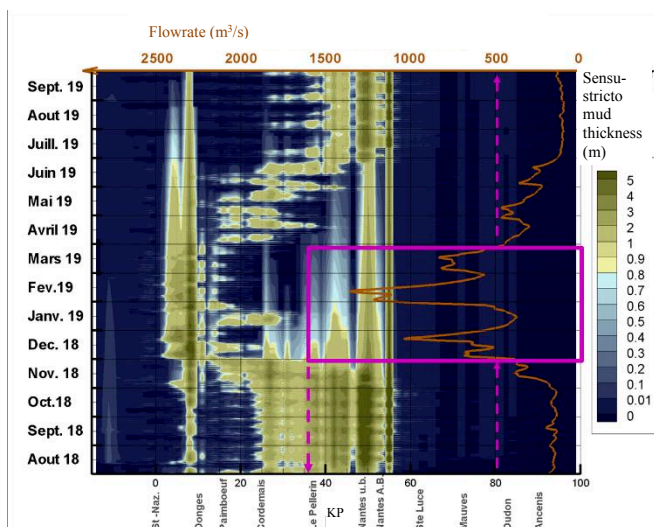


Figure 11. Modelled annual dynamic of fluid mud

### III. LOCAL DUMPING MODEL

The port is dredging sediments from the navigation channel and then dumping it at the Lambarde dumping site. Evolution of bottom elevation at the site and assessing the stability rate of the area can help defining dumping scenarios for future operations. The aim of this local model is to represent the bottom evolutions of each dumping sub-zone, and the global sediment volume that consolidates over time, compared to the dumped volume.

#### A. Model set up

To achieve this goal, a new mesh is created, highly refined around the dumping area. The model boundary nodes correspond exactly to nodes from the global hydrosedimentary model. This allows us to force our local “sub-model” with results from the global model, for the hydrodynamics part. Waves’ parameters are still extracted from the HOMERE database. Wind is not taken into account anymore, to reduce computational times, and because levels imposed at the boundary already include wind effects. In addition to the forcing data of the global hydrosedimentary model, dumped sediment mass is taken into account. All the dumping operations are integrated in the model one by one, and with respect to the real chronological order. A map of every dumping “sub-zone” and the time period associated is shown in Figure 12.

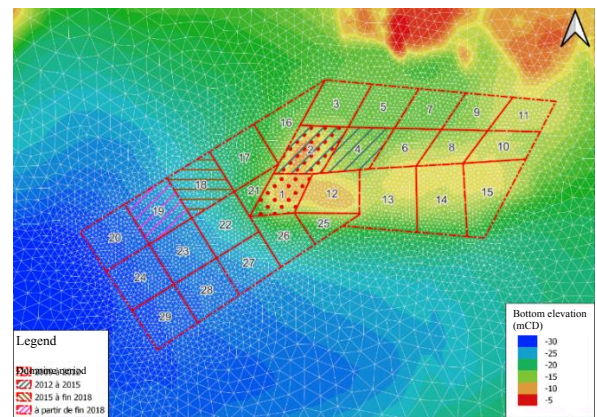


Figure 12. Dumpings sub-zones and time period associated

#### B. Dumpings modelling

Usually, one would distinct three different phases in the dumping: suspension, bottom deposit, and bottom turbid plume. On this local model, bottom turbid plume is not predefined with parameters, but derives from the suspended sediment fall. This gives more realistic results than when you impose the turbid plume with a predefined geometry.

Mass repartition inside the two phases is fixed after calibration at: 100% bed deposit for sand, 60% suspension and 40% bed deposit for mud. The suspended part is injected uniformly thanks to source terms in each of the horizontal plane of the 3D-model. The bed deposit is modelled in a way that it represents the crater geometry that is observed in-situ. In the model, it depends of three parameters, as shown in the Figure 13.



The different radii are used to:

- R1: handle size of inner crater;
- R2: handle size of footprint;
- R3: handle mass repartition inside the geometry

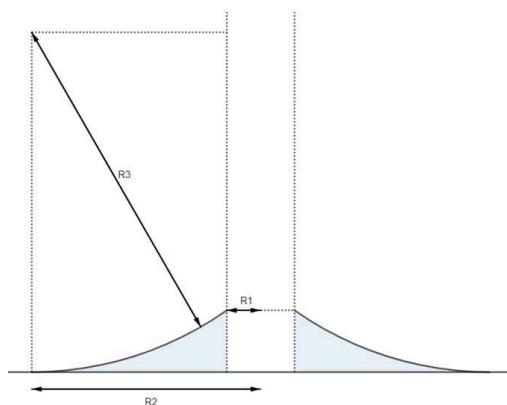


Figure 13. Geometry of ground deposit

The sediment mass that composes this deposit is added into layers of the bed model. The layers are adapted during the calibration phase, to find the best repartition to properly reproduce in-place volume and sub-zone elevations.

C. Results and discussion

The local model of the Lambarde dumping site is calibrated over around 9 years, from September 2011 to May 2020. During this calibration, bed deposit geometry, suspension percentage for mud, layers chosen for bed deposit and critical slope for sliding were adapted to properly reproduce both the temporal evolution of the global volume on the area, and the temporal evolution of mean elevations for every sub-zone. Data for mean elevations and volume is calculated from the different bathymetric set available (around 1 per year). Uncertainty in the calculated volume can thus be quite high, depending on the bathymetry uncertainty (which is never below 0.1 meters in our case).

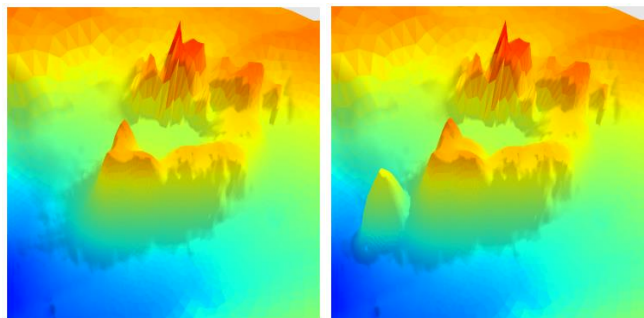


Figure 14. Model bathymetry at the start of the simulation (left) and after 9 years of dumping (right)

The Figure 14 shows a 3D view of the dumping site at the start of the simulation, and after the 9 years of dumping.

The main objective is to reproduce the global evolution of the site, with good correlation between model and

measurements as far as volume is concerned. The final results obtained are shown in the Figure 15.



Figure 15. Calibration result for in-place volume – Model in red line, dumped volume in green line and in-place volume data in blue dots

Stability of the site which is the ratio between the deposited volume and the dumped volume, is calculated for different representative dumping periods. Table III summarizes modelled stability rates versus in-situ ones.

Table III – In-situ and modelled stability rates

	09/2011 → 09/2019	09/2011 → 05/2015	05/2015 → 06/2018	06/2018 → 07/2019
<b>In-situ</b>	18.7 %	10.5 %	26 %	13.3 %
<b>Modelled</b>	18.4 %	11.4 %	25.4 %	7.6 %

As far as elevations are concerned, a good calibration shows the capability of the model to reproduce the spreading of the deposit, and the erosion flux during period where no dumping is done. Final results for mean elevations are shown in Figure 16.

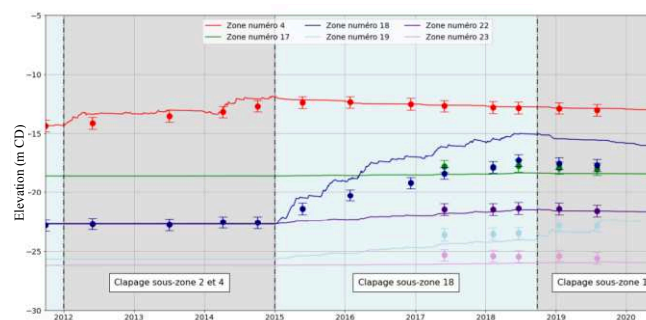


Figure 16. Calibration results for mean elevations. Model in plain lines and data in dots.

IV. CONCLUSION AND PERSPECTIVES

A global 3D hydrosedimentary model of the Loire estuary has been built up and calibrated with diverse data and on diverse periods. So far, the model shows good capability to represent the large scale dynamics of sediment transport, or fluid mud movement. A local dumping model of the Lambarde site has also been built and calibrated. It reproduces quite well the stability of the dumping site, over

10 years, and also over a sub-zone dumping period. The global model is currently being improved by adding:

- The modelling of dredging processes inside the estuary. The local dumping model will be included inside the global mesh, and refinement will be made on the coastal at the mouth of the estuary, with a goal to reproduce dispersion of sediments after the dumping process. Mass-balance inside the whole estuary will be at stake;
- A water quality module, using WAQTEL.

It should in the end provide answers to a lot of hydraulic related topics that stakeholders can be interested in. The information provided by this model is even more important when facing harsh natural phenomena such as the draught that happened this summer, and to which we should be more and more subject in the future.

#### ACKNOWLEDGEMENT

Authors acknowledge the GIP Loire Estuaire for funding the study and for all the data provided.

#### REFERENCES

- [1] Sanchez M., Grimigni P et Delanoe Y.,2004. "Distribution des sédiments cohésifs en relation avec la vitesse de la phase solide dans l'estuaire de la Loire , VIII journées Nationales Génie Civil-Génie Côtier, Compiègne 7 et 9 septembre 2007"
- [2] Sanchez M., Levacher D.,2008. "Erosion d'une vase de l'estuaire de la Loire sous l'action du courant", Bull Eng Envir (2008) 67, p597
- [3] Van Rijn, L. 2007. Unified View of Sediment Transport by Currents and Waves. Journal of Hydraulic Engineering, ASCE / June 2007
- [4] European Marine Observation and Data network: <http://www.emodnet-geology.eu/>
- [5] Carrère L., F. Lyard, M. Cancet, A. Guillot, L. Roblou, FES2012: A new global tidal model taking taking advantage of nearly 20 years of altimetry, *Proceedings of meeting "20 Years of Altimetry"*, Venice 2012
- [6] GIPLE, cahier indicateurs numéro 1, fiche L1E2, Avril 2014 : [https://www.loire-estuaire.org/accueil/actualites/10\\_52198/nouvelle\\_fiche\\_de\\_synthese\\_l1e2\\_la\\_dynamique\\_du\\_bouchon\\_vaseux](https://www.loire-estuaire.org/accueil/actualites/10_52198/nouvelle_fiche_de_synthese_l1e2_la_dynamique_du_bouchon_vaseux)
- [7] Walther R, Schaguene J, Hamm L, David E, Coupled 3D modeling of turbidity maximum dynamics in the Loire estuary., Coastal Engineering Proceedings, 1(33), ICCE 2012– Santander, Spain, 06/2012
- [8] Thorn, M. F. C. (1982), Physical processes of siltation in tidal channels, in Hydraulic Modelling in Maritime Engineering: Proceedings of the Conference/Organized by the Institution of Civil Engineers, Held in London on 13 – 14 October 1981, pp. 47 – 55, Thomas Telford, London